Nodal and Nematic Superconducting Phases in NbSe$_2$ Monolayers from Competing Superconducting Channels

Chang-woo Cho,[1] Jian Lyu,[1,2] Liheng An,[1] Tianyi Han,[1] Kwan To Lo,[1] Cheuk Yin Ng,[1] Jiaqi Hu,[1]
Yuxiang Gao,[1] Gaomin Li,[2] Mingyuan Huang,[2] Ning Wang,[1] Jörg Schmalian,[3] and Rolf Lortz[1,*]

[1]*Department of Physics, The Hong Kong University of Science and Technology, Clear Water Bay, Kowloon, Hong Kong*
[2]*Department of Physics, Southern University of Science and Technology,
1088 Xueyuan Road, Nanshan District, 518000 Shenzhen, Guangdong Province, China*
[3]*Institute for Theory of Condensed Matter and Institute for Quantum Materials and Technologies,
Karlsruhe Institute of Technology, 76131 Karlsruhe, Germany*

Transition metal dichalcogenides like 2H-NbSe$_2$ in their two-dimensional (2D) form exhibit Ising superconductivity with the quasiparticle spins being firmly pinned in the direction perpendicular to the basal plane. This enables them to withstand exceptionally high magnetic fields beyond the Pauli limit for superconductivity. Using field-angle-resolved magnetoresistance experiments for fields rotated in the basal plane we investigate the field-angle dependence of the upper critical field (H_{c2}), which directly reflects the symmetry of the superconducting order parameter. We observe a sixfold nodal symmetry superposed on a twofold symmetry. This agrees with theoretical predictions of a nodal topological superconducting phase near H_{c2}, together with a nematic superconducting state. We demonstrate that in NbSe$_2$ such unconventional superconducting states can arise from the presence of several competing superconducting channels.

2H-NbSe$_2$ is a layered transition metal dichalcogenide (TMDC) superconductor with bulk critical temperature $T_c = 7.2$ K and remains superconducting in monolayer form [1,2]. The layers have honeycomb lattice structure with broken A-B sublattice and inversion symmetry and heavy transition metal atoms causing strong spin-orbit coupling (SOC) [3–5]. The electrons experience in-plane electric fields from a broken in-plane mirror symmetry, which leads to an Ising SOC field [6] and pins the electron spins to the out-of-plane direction [7–9]. Cooper pairs are not affected by the Pauli limit and can exist in high magnetic fields parallel to the layers [1,6]. Such Ising superconductivity in monolayer NbSe$_2$ has been predicted to feature a topological superconducting phase with six pairs of point nodes [10–12], protected by time-reversal symmetry and connected by Majorana arcs [13–15]. In this Letter, we investigate the pairing gap symmetry of NbSe$_2$ monolayers by field-angle-resolved electric transport measurements in strictly parallel fields. The angular H_{c2} dependence directly reflects the superconducting order parameter symmetry [16,17]. We find that the in-plane field drives the superconductor into an unconventional state, with the predicted sixfold nodal symmetry [10], and a nematic phase [18] consisting of a primary single-component order parameter competing with a subleading unconventional two-component order parameter.

In total three monolayer samples have been studied with consistent results in comparison to thicker samples in which the effects were much weaker. The 2D NbSe$_2$ samples were fabricated using the standard exfoliation method onto a hexagonal boron-nitride layer on a SiO$_2$/Si substrate with 15 nm deep grooves cut by plasma etching and filled with Au to form nonprotruding bottom electrodes. NbSe$_2$ flakes were exfoliated onto PMMA and transferred onto the substrate, keeping the PMMA as a protective layer. Figure 1(a) shows an optical image of sample 1 where a monolayer flake is connected by five terminals. Micro-Raman spectroscopy was used to confirm the presence of a monolayer region between the
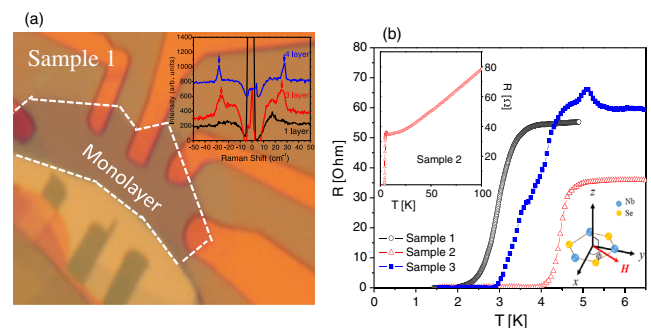

FIG. 1. (a) Optical image of sample 1 showing the monolayer region. The inset shows local Raman spectra at different positions used to identify the monolayer region. The spectra were shifted vertically. (b) Zero-field electrical resistance of our three monolayer devices. The left inset shows data up to 100 K. The right inset defines the in-plane field orientation in the honeycomb lattice with respect to the x axis (angle ϕ).

087002-1

terminals [19]. Electrical magnetotransport measurements were performed with a standard four-probe ac method. The devices were mounted on a piezorotatory stage with its axis perpendicular to the field. Exact parallel field alignment of the $NbSe_2$ layers was secured by a goniometer. Figure 1(b) shows the zero-field T_c of monolayer samples 1–3, which varies between 3 and 4.4 K, attributed to subtle differences in the preparation of the devices: monolayers are a delicate material whose properties are strongly influenced by external parameters such as the substrate material [2], wrinkles, and strains [21].

In Fig. 2(a), we plot 12-T resistance data for sample 1 for different in-plane field angles Φ [Fig. 1(b)]. A significant angular variation is observed. We marked characteristic temperatures at which the resistance reaches 50% of the normal state resistance R_N and 90% R_N within the superconducting transition by stars. Figures 2(b) and 2(c) show their Φ dependence. At 90% R_N, it shows a pronounced sixfold variation with sharp kinks each 60° superimposed

by a twofold variation. At 50% R_N, the kinks are less evident, and the twofold symmetry dominates.

Figure 2(d) shows Φ dependence of the characteristic temperatures where 90% R_N is reached for sample 2 and Fig. 2(e) for 50% R_N (see Supplemental Material [19] for resistance data), showing a similar trend. At 90% R_N, just before the sample enters the normal state, the angular dependence shows a sixfold variation with even more pronounced sharp spikelike maxima at 60°, 120°, and 180°, superimposed by a weaker twofold variation. At lower temperatures (50% R_N), the spikes disappear, and the data show a strong twofold symmetry.

For sample 3 we obtained better results in measuring the magnetoresistance (MR) at fixed temperatures (2.3 and 3.7 K), as a function of the magnetic field (see Ref. [19] for the original MR data), allowing us to derive characteristic fields related to H_{c2} [19]. At 3.7 K, $H_{c2}(\Phi)$ [Fig. 2(f)] taken as the field where 90% or R_N is reached, shows very similar peaks with sixfold rotational symmetry, while at
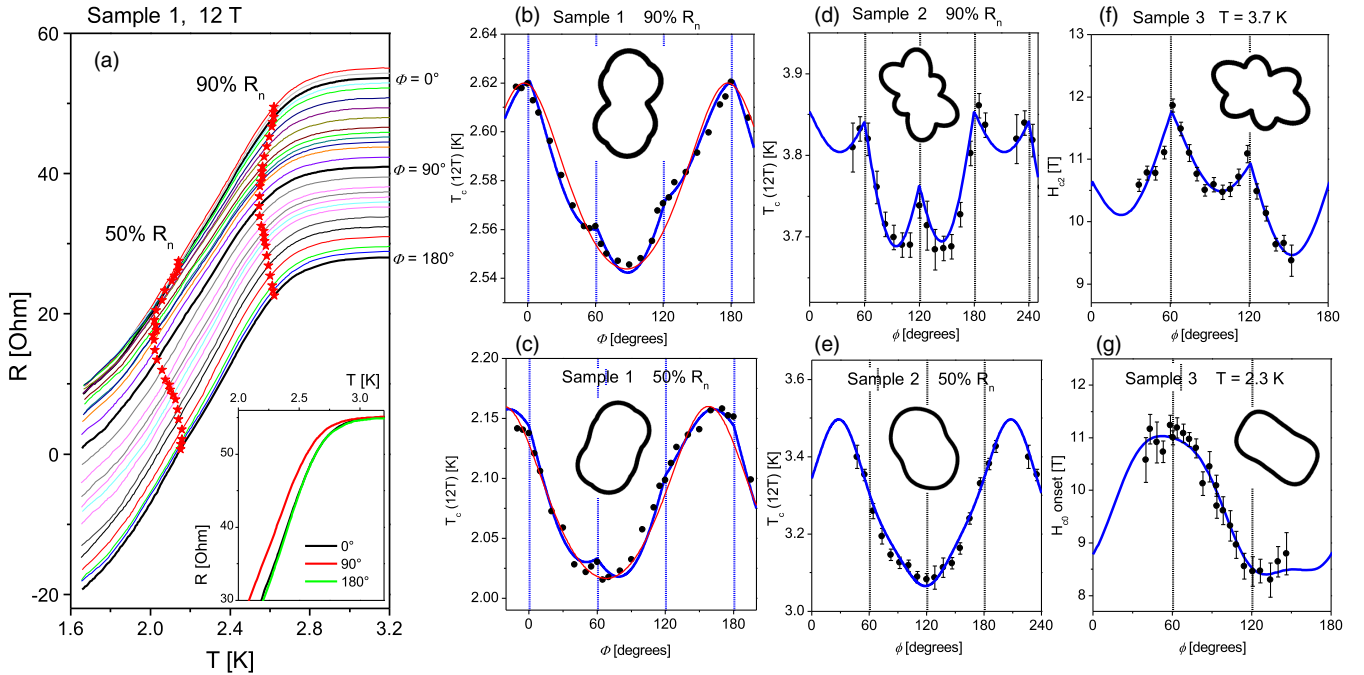

FIG. 2. (a) Resistance of sample 1 in a 12 T magnetic field of different in-plane orientations $\phi = -10°, -5°, 0°, 5°, 10°, 15°, 20°, 30°, 40°, 50°, 55°, 60°, 65°, 70°, 80°, 90°, 100°, 110°, 115°, 120°, 125°, 130°, 140°, 150°, 160°, 170°, 175°,$ and $180°$. Offsets were added except for $\phi = -10°$. The inset shows 0°, 90°, and 180° data without offsets. The stars mark temperatures at which 90%, and 50% of R_N is reached. (b),(c) ϕ dependence of the two characteristic temperatures marked in (a), which illustrate the symmetry of $T_c(12\,T)$. Blue lines are fitting functions for a sixfold nodal symmetry and a twofold nematic symmetry (see text for details). The red lines only consider a twofold nematic symmetry and fail to describe the kink structures. (d), (e) Similarly obtained ϕ dependence of sample 2 for 90% and 50% of R_N [see Supplemental Material, Fig. 2 [19]]. The lines are fitting functions for a sixfold nodal symmetry (d), a sixfold sinusoidal symmetry (e), and twofold nematic symmetries (d), (e). (f) ϕ dependence of H_{c2} obtained from magnetoresistance data of sample 3 at 3.7 K [see Supplemental Material, Fig. 3(b) [19]] at 90% of R_N. The line is a fitting function for a sixfold nodal symmetry and weak twofold nematic symmetry. (g) ϕ dependence of the characteristics critical field H_{c0} onset, above which zero resistance is lost, from sample 3 at 2.3 K [Supplemental Material, Fig. 3(a) [19]]. The line is a fitting function for a weak sixfold sinusoidal variation and a twofold nematic symmetry. The insets in Figs. 2(b)–2(g) illustrate the symmetry of the order parameter derived from the representation of the reciprocals of the fitting functions in a polar diagram.
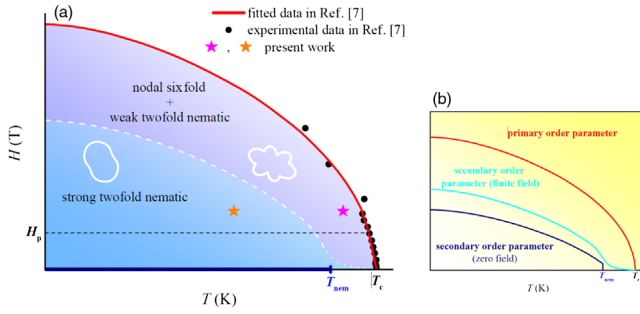
FIG. 3. (a) Magnetic field vs temperature phase diagram. The horizontal line marks the Pauli limit H_P. The stars mark the regions in which we observe a sixfold nodal or a twofold nematic order parameter symmetry. (b) Temperature dependence of the primary and secondary order parameter of the nematic superconducting state.

2.3 K [Fig. 2(g)] shows the characteristic field H_{c0} onset, above which the zero resistance is lost [Supplemental Material [19], Fig. 3(b)], shows a pronounced twofold symmetry. The behavior of all three devices (sample 1– sample 3) is similar, which demonstrates the reproducibility.

To evaluate the ϕ variations of the characteristic temperatures or fields, we used Eqs. (1) and (2) as fitting functions. The first term describes a twofold nematic symmetry [22] to which we add a $|\cos(3\phi + \phi_6)|$ term [Eq. (1)] to model a sixfold nodal symmetry with its sharp peaks, or a smooth sinusoidal variation of a nodeless sixfold symmetry [Eq. (2)].

$$H_{c2}(\phi) = \frac{A_2}{\sqrt{\cos^2(\phi + \phi_2) + \Gamma^2 \sin^2(\phi + \phi_2)}} + A_6 |\cos(3\phi + \phi_6)|, \tag{1}$$

$$H_{c2}(T, \phi) = \frac{A_2}{\sqrt{\cos^2(\phi + \phi_2) + \Gamma^2 \sin^2(\phi + \phi_2)}} + A_6 \cos(6\phi + \phi_6). \tag{2}$$

Γ is the anisotropy parameter, A_i and ϕ_i ($i = 2, 6$) indicate the gap amplitude and phase. Note that while these equations describe the anisotropy for $H_{c2}(T, \phi)$, our temperature dependent resistance data provide $T_c(H, \phi)$, which is directly related to $H_{c2}(T, \phi)$ and follows the same ϕ dependence. The fitting functions [Eq. (1)] are included as lines in Fig. 2. A nodal sixfold gap function is required to describe the kinks near the normal state boundary Figs. 2(b), 2(d), and 2(f). In addition, a twofold variation must be considered. For samples 2 and 3 the kinks are only evident in the vicinity of the normal state boundary Figs. 2(d) and 2(f), while further in the superconducting phase Eq. (2) describes the data better Figs. 2(e) and 2(g). Maxima in the Φ dependence of H_{c2} correspond to order parameter minima. To illustrate the in-plane order parameter, we have inserted small polar plots [19] of the

reciprocals of the fits Figs. 2(b)–2(g). The symmetries in Figs. 2(b), 2(d), and 2(f) with its six lobes resemble a distorted $4f_{x-3xy}^3{}^2$ orbital with three line nodes in the plane, which cannot be distinguished from the predicted six pairs of point nodes. Inside the superconducting phase the symmetries approach a twofold nematic symmetry with only a small sixfold sinusoidal distortion.

Discussion.—Our observation of a sixfold sharp kinklike dependence of $H_{c2}(T, \phi)$ matches the theoretically prediction of a nodal superconducting phase [10], although our experiment suggests that its existence is limited to a small region near the normal state boundary. The additional twofold variation contradicts the trifold crystalline in-plane symmetry and can be regarded as a nematic superconductivity [18]. Our studies on thicker samples revealed that the strong anisotropies are exclusively found in NbSe$_2$ monolayers, while multilayers had much weaker anisotropies [19]. Nematic superconductivity means that a rotational symmetry breaking occurs near the onset of superconductivity. Artifacts due to misalignment of the sample surface with respect to the axis of rotation can be excluded [19], since the parallel alignment was carefully monitored and adjusted. Furthermore, in none of our devices a correlation between the current direction and the observed twofold symmetry existed [19], which excludes anisotropies due to dissipation from vortices [23]. In the inset of Fig. 2(a), the 12T-resistance data coincide for 0° and 180°, but the 90° data are shifted to lower temperature without changing shape, which demonstrates that the anisotropy originates from a true H_{c2} anisotropy and not solely from a variation of the sheet resistance. For sample 1 the orientation of the twofold symmetry varies even slightly as a function of temperature, and we found that in the region between contacts 1 and 2 the orientation is different, which suggests the presence of different nematic domains [19]. Superconductivity and incommensurate CDW ordering have been reported to coexist in monolayers [24], but a microscopic model showed that density wave instabilities decouple from the SC channels [12] and are exponentially suppressed. It is therefore unlikely that density waves are related to the nodal features. Moreover, the nematic twofold orientation is not obviously connected to the crystalline lattice and therefore cannot be caused by density waves.

In Fig. 3(a) we summarize our results in an H-T phase diagram. We observe the kinks of the sixfold rotational symmetry for all monolayer samples near the normal state boundary. At lower temperatures and fields, the kinks become less evident (sample 1) or absent (samples 2 and 3) [19], and the field angle dependence is dominated by the twofold symmetry. Our transport data do not provide information in the zero-resistance region, but the additional twofold rotational symmetry attributed to nematic superconductivity is observed wherever the resistance remains finite.

NbSe$_2$ monolayers are subject to a strong Ising SOC and a Zeeman field in the plane. The broken inversion

symmetry in the crystal symmetry causes a mixture of spin singlet and triplet pairing potential [18,22,25]. The interplay between the Zeeman field, SOC, and disorder is regarded to be crucial for tuning the coupling among the different pairing channels [26]. The nodes represent six pairs of point nodes on the two Γ pockets along the three Γ-M lines in the Brillouin zone [10]. Ising SOC is absent along these directions, so the Zeeman energy can exceed the pairing energy of the spin-singlet Cooper pairs, thus closing the gap and forming point nodes [10]. It has been shown [12] that there are two instabilities in singlet and triplet interaction channels leading to a crystalline topological superconducting phase, which involves the nodal phase [10]. Such a nodal crystalline topological superconducting phase has particle-hole symmetry and an antiunitary time-reversal-like symmetry, the latter being a composition of time-reversal symmetry and a reflection with respect to the xy plane [12].

The theoretical framework for the nodal superconducting phase is readily available in the literature [10,12], but the observed differences in the phase diagram with the additional nematic phase require further theoretical analysis. Theory assumes that the nodal phase occurs in a large region above the Pauli limit, while we find that the nodal phase is confined to a narrow region near the normal state boundary, being replaced by the nematic phase deeper within the SC state. In the following, we present a scenario that naturally accounts for the observation of the two unusual phases because of the presence of multiple competing superconducting channels in NbSe$_2$ monolayers: a dominant single-component (likely s-wave) pairing state and a subleading, unconventional two-component order parameter, which leads to nematicity because of the symmetry-permitted nonlinear coupling between both pairing states [Fig. 3(b)].

In a nematic superconductor, the onset of superconductivity not only breaks the global U(1) symmetry of the pairing state, but also a discrete rotational symmetry of the crystal lattice, which can even occur above the actual superconducting phase transition [27–29]. The superconducting order parameter must then transform according to a higher-dimensional irreducible representation of the point group. The point group of freestanding monolayer NbSe$_2$ is D_{3h}. On a substrate, the horizontal mirror plane disappears, and the resulting group becomes C_{3v}. In C_{3v} there is a 2D irreducible representation E with leading polynomials (k_x, k_y), or $(k_x^2-k_y^2, k_x k_y)$. A superconductor that orders according to this E representation would then be characterized by

$$\Delta_{\alpha\beta}(k) = \psi_1\left(\Delta_{x^2-y^2}(\boldsymbol{k}) + \boldsymbol{d}_x(\boldsymbol{k}) \cdot \boldsymbol{\sigma}\right)i\sigma_y$$
$$+ \psi_2\left(\Delta_{xy}(\boldsymbol{k}) + \boldsymbol{d}_y(\boldsymbol{k}) \cdot \boldsymbol{\sigma}\right)i\sigma_y. \quad (3)$$

Here, $\Delta_{\alpha\beta}(\boldsymbol{k}) = \langle c_{k\alpha}c_{-k\beta}\rangle$ describes the Cooper pair with crystal momentum $\boldsymbol{k}$ and spin α, β. $\Delta_{x^2-y^2}(\boldsymbol{k}) \propto \cos k_x - \cos k_y$ and $\Delta_{xy}(\boldsymbol{k}) \propto \sin k_x \sin k_y$ describe singlet pairing

amplitudes while the $\boldsymbol{d}_{x,y}(\boldsymbol{k})$ describe the triplet component, which is allowed given the broken inversion symmetry at the interface. The pairing is then characterized by the two-component order parameter $\psi = (\psi_1, \psi_2)$. A nematic state has the helical form $(\psi_1, \psi_2) \propto (\cos\theta, \sin\theta)$. An immediate concern is that one would then expect pairing states in bulk NbSe$_2$ that naturally merge with the E representation on the surface, given that the bulk and surface transition temperatures are comparable. These pairing states would then be either of E_{2g} or E_{1u} symmetry with the bulk point group D_{6h}. There seems to be no evidence for such behavior in bulk NbSe$_2$. Another, arguably more fundamental objection against primary nematic superconductivity in monolayer NbSe$_2$ follows from the analysis of Ref. [30], where monolayers with broken inversion symmetry were considered in the limit where the spin splitting due to the inversion symmetry breaking is larger than the superconducting gap, a condition which is satisfied. It has been shown that superconductivity with higher-dimensional irreducible representations, such as E, always breaks time reversal symmetry, i.e., $(\psi_1, \psi_2) \propto (1, \pm i)$, instead of being nematic.

A natural explanation for the observed behavior is that the primary superconducting order parameter φ is a single-component degree of freedom. However, in addition to this primary superconducting order parameter, pairing in the E-symmetry channel, i.e., with the pairing wave function given in Eq. (3) with the two-component order parameter $\psi = (\psi_1, \psi_2)$, is a close contender. Then, the symmetry properties at the interface allow a phase transition $T_{\text{nem}} < T_c$ at zero field [Fig. 3(a)], where ψ becomes finite and enters a nematic state [Fig. 3(b)]. This nematic order is a direct consequence of the nonlinear coupling between the two almost degenerated order parameters. The most conservative choice would be s pairing in the A_1 symmetry. Then a coupling of the type

$$f_{\text{int}} = \frac{g}{4}\left[\varphi^*(\psi_1|\psi_1|^2 - \psi_2\psi_1^*\psi_2 - 2\psi_1|\psi_2|^2) + \text{H.c.}\right] \quad (4)$$

is symmetry allowed and induces a nematic state which is either $\psi^{(1)} = \psi_0(1,0)$, $\psi^{(2)} = \psi_0[-\frac{1}{2}, (\sqrt{3}/2)]$, or $\psi^{(3)} = \psi_0[-\frac{1}{2}, -(\sqrt{3}/2)]$ with amplitude $\psi_0 \propto \varphi$ below a first order transition at T_{nem}. A similar behavior occurs if φ is odd under vertical mirror reflections, i.e., an A_2 order parameter, which yields instead

$$f_{\text{int}} = \frac{g}{4}\left[\varphi^*(\psi_2|\psi_2|^2 - \psi_1\psi_2^*\psi_1 - 2\psi_1\psi_1^*\psi_2) + \text{H.c.}\right] \quad (5)$$

with similar nematic order. These nematic states occur for a sufficiently large coupling constant g, even though the secondary order parameter ψ prefers, on its own, a chiral state with time-reversal symmetry breaking [30]. Interestingly, a coupling term like Eq. (4) has recently been

discussed in the context of nematic superconductivity in twisted bilayer graphene [31].

If there are two almost degenerated order parameters that transform simultaneously under A_1 and E, an in-plane magnetic field plays an important role in mixing these two states below T_c [Fig. 3(b)]. This is a consequence of the magnetic field induced bilinear coupling between the two order parameters, which induces the nematic state anywhere below T_c. Only directly at the transition temperature are nematic effects absent, which explains the observed sixfold symmetry. Our analysis demonstrates that the nematic phase competes with the nodal phase so that it becomes confined to a relatively small region near the normal state boundary, in contrast to Ref. [10] where the nodal phase was predicted over a much larger field and temperature range. Upon entering the superconducting state, one first enters the nodal phase, which is then replaced by the nematic phase. It would be interesting to see if there is a phase transition line separating the two states, even though our data tend to suggest a rather smooth crossover. This magnetic field coupling term is even under time reversal, gauge invariant and compatible with all point symmetries. The physics underlying this coupling was recently discussed in Ref. [26].

Our detailed field-angle-resolved study of the H_{c2} transition in 2D NbSe$_2$ samples revealed two distinct unconventional superconducting phases in high parallel fields, both being a consequence of competing superconducting channels. The sixfold nodal phase agrees with the prediction of a topological superconducting phase [10]. The additional twofold symmetry reveals that this material is characterized by a primary order parameter, likely of s-wave nature, and a two-component close competitor that transforms according to a nontrivial symmetry. The nonlinear coupling between them induces a nematic state at $T_{\mathrm{nem}} < T_c$ and pins a twofold symmetry axis in the system. An in-plane magnetic field induces nematic order at temperatures even above T_{nem}, all the way up to T_c. A role of strain in determining the pinning direction of the twofold anisotropy is likely. In doped Bi$_2$Se$_3$ [29], intrinsic strain from a separate nematic transition above T_c is crucial in aligning the direction of the anisotropic gap along a particular in-plane direction. For 2D NbSe$_2$, the strain field is likely extrinsic from the exfoliation process.

Note added.—Recently, we became aware of a preprint that reported a similar twofold breaking of rotational symmetry in few-layer NbSe$_2$ [32].

*Corresponding author.
lortz@ust.hk

[1] X. Xi, Z. Wang, W. Zhao, J.-H. Park, K. T. Law, H. Berger, L. Forró, J. Shan, and K. F. Mak, Ising pairing in superconducting NbSe$_2$ atomic layers, Nat. Phys. **12,** 139 (2016).

[2] M. M. Ugeda, A. J. Bradley, Y. Zhang, S. Onishi, Y. Chen, W. Ruan, C. Ojeda-Aristizabal, H. Ryu, M. T. Edmonds, H.-Z. Tsai, A. Riss, S.-K. Mo, D. Lee, A. Zettl, Z. Hussain, Z.-X. Shen, and M. F. Crommie, Characterization of collective ground states in single-layer NbSe$_2$, Nat. Phys. **12,** 92 (2016).

[3] Z. Y. Zhu, Y. C. Cheng, and U. Schwingerschlögl, Giant spin-orbit-induced spin splitting in two-dimensional transition-metal dichalcogenide semiconductors, Phys. Rev. B **84,** 153402 (2011).

[4] D. Xiao, G.-B. Liu, W. Feng, X. Xu, and W. Yao, Coupled Spin and Valley Physics in Monolayers of MoS$_2$ and Other Group-VI Dichalcogenides, Phys. Rev. Lett. **108,** 196802 (2012).

[5] A. Kormányos, V. Zólyomi, N. D. Drummond, P. Rakyta, G. Burkard, and V. I. Fal'ko, Monolayer MoS$_2$: Trigonal warping, the Γ valley, and spin-orbit coupling effects, Phys. Rev. B **88,** 045416 (2013).

[6] J. M. Lu, O. Zheliuk, I. Leermakers, N. F. Q. Yuan, U. Zeitler, K. T. Law, and J. T. Ye, Evidence for two-dimensional Ising superconductivity in gated MoS$_2$, Science **350,** 1353 (2015).

[7] N. F. Q. Yuan, K. F. Mak, and K. T. Law, Possible Topological Superconducting Phases of MoS$_2$, Phys. Rev. Lett. **113,** 097001 (2014).

[8] M. Rösner, S. Hass, and T. O. Wehling, Phase diagram of electron-doped dichalcogenides, Phys. Rev. B **90,** 245105 (2014).

[9] R. Roldán, E. Cappelluti, and F. Guinea, Interactions and superconductivity in heavily doped MoS$_2$, Phys. Rev. B **88,** 054515 (2013).

[10] W.-Y. He, B. T. Zhou, J. J. He, N. F. Q. Yuan, T. Zhang, and K. T. Law, Magnetic field driven nodal topological superconductivity in monolayer transition metal dichalcogenides, Commun. Phys. **1,** 40 (2018).

[11] M. H. Fischer, M. Sigrist, and D. F. Agterberg, Superconductivity without Inversion and Time-Reversal Symmetries, Phys. Rev. Lett. **121,** 157003 (2018).

[12] D. Shaffer, J. Kang, F. J. Burnell, and R. M. Fernandes, Crystalline nodal topological superconductivity and Bogolyubov Fermi surfaces in monolayer NbSe$_2$, Phys. Rev. B **101,** 224503 (2020).

[13] S.-Y. Xu *et al.*, Discovery of a Weyl fermion semimetal and topological Fermi arcs, Science **349,** 613 (2015).

[14] H. Weng, C. Fang, Z. Fang, B. A. Bernevig, and X. Dai, Weyl Semimetal Phase in Noncentrosymmetric Transition-Metal Monophosphides, Phys. Rev. X **5,** 011029 (2015).

[15] L. X. Yang, Z. K. Liu, Y. Sun, H. Peng, H. F. Yang, T. Zhang, B. Zhou, Y. Zhang, Y. F. Guo, M. Rahn, D. Prabhakaran, Z. Hussain, S.-K. Mo, C. Felser, B. Yan, and Y. L. Chen, Weyl semimetal phase in the non-centrosymmetric compound TaAs, Nat. Phys. **11,** 728 (2015).

[16] K. Machida, M. Ozaki, and T. Ohmi, Unconventional superconducting class in a heavy fermion system UPt$_3$, J. Phys. Soc. Jpn. **58,** 4116 (1989).

[17] K. Machida, T. Ohmi, and M. Ozaki, Anisotropy of upper critical fields for d- and p-wave pairing superconductivity, J. Phys. Soc. Jpn. **54**, 1552 (1985).

[18] For a recent review, see, e.g., S. Yonezawa, Nematic superconductivity in doped Bi_2Se_3 topological superconductors, Condens. Matter **4**, 2 (2019).

[19] See Supplemental Material at http://link.aps.org/supplemental/10.1103/PhysRevLett.129.087002 for additional supporting data and discussion of some details, which includes Ref. [20].

[20] Y. Xing et al., Ising superconductiviy and quanum phase transition in macro-size monolayer $NbSe_2$, Nano Lett. **17**, 6802 (2017).

[21] C. Chen, P. Das, E. Aytan, W. Zhou, J. Horowitz, B. Satpati, A. A. Balandin, R. K. Lake, and P. Wei, Strain-controlled superconductivity in few-layer $NbSe_2$, ACS Appl. Mater. Interfaces **12**, 38744 (2020).

[22] J. Shen, W.-Y. He, N. F. Q. Yuan, Z. Huang, C.-w. Cho, S. H. Lee, Y. S. Hor, K. T. Law, and R. Lortz, Nematic topological superconducting phase in Nb-doped Bi_2Se_3, npj Quantum Mater. **2**, 59 (2017).

[23] Y.-L. Wang, A. Glatz, G. J. Kimmel, I. S. Aranson, L. R. Thoutam, Z.-L. Xiao, G. R. Berdiyorov, F. M. Peeters, G. W. Crabtree, and W.-K. Kwok, Parallel magnetic field suppresses dissipation in superconducting nanostrips, Proc. Natl. Acad. Sci. U.S.A. **114**, E10274 (2017).

[24] Y. Nakata, K. Sugawara, S. Ichinokura, Y. Okada, T. Hitosugi, T. Koretsune, K. Ueno, S. Hasegawa, T. Takahashi, and T. Sato, Anisotropic band splitting in monolayer $NbSe_2$: Implications for superconductivity and charge density wave, npj 2D Mater. Appl. **2**, 12 (2018).

[25] P. A. Frigeri, D. F. Agterberg, A. Koga, and M. Sigrist, Superconductivity without Inversion Symmetry: MnSi versus $CePt_3Si$, Phys. Rev. Lett. **92**, 097001 (2004).

[26] D. Möckli and M. Khodas, Ising superconductors: Interplay of magnetic field, triplet channels, and disorder, Phys. Rev. B **101**, 014510 (2020).

[27] M. Hecker and J. Schmalian, Vestigial nematic order and superconductivity in the doped topological insulator $Cu_xBi_2Se_3$, npj Quantum Mater. **3**, 26 (2018).

[28] R. M. Fernandes, P. P. Orth, and J. Schmalian, Intertwined vestigial order in quantum materials: Nematicity and beyond, Annu. Rev. Condens. Matter Phys. **10**, 133 (2019).

[29] C.-w. Cho, J. Shen, J. Lyu, O. Atanov, Q. Chen, S. H. Lee, Y. S. Hor, D. J. Gawryluk, E. Pomjakushina, M. Bartkowiak, M. Hecker, J. Schmalian, and R. Lortz, Z_3-vestigial nematic order due to superconducting fluctuations in the doped topological insulators $Nb_xBi_2Se_3$ and $Cu_xBi_2Se_3$, Nat. Commun. **11**, 3056 (2020).

[30] M. S. Scheurer, D. F. Agterberg, and J. Schmalian, Selection rules for Cooper pairing in two-dimensional interfaces and sheets, npj Quantum Mater. **2**, 9 (2017).

[31] D. V. Chichinadze, L. Classen, and A. V. Chubukov, Nematic superconductivity in twisted bilayer graphene, Phys. Rev. B **101**, 224513 (2020).

[32] A. Hamill, B. Heischmidt, E. Sohn, D. Shaffer, K.-T. Tsai, X. Zhang, X. Xi, A. Suslov, H. Berger, L. Forró, F. J. Burnell, J. Shan, K. F. Mak, R. M. Fernandes, K. Wang, and V. S. Pribiag, Two-fold symmetric superconductivity in few-layer $NbSe_2$, Nat. Phys. **17**, 949 (2021).